Atmos. Chem. Phys., 23, 15197–15207, 2023
https://doi.org/10.5194/acp-23-15197-2023

Atmospheric Chemistry and Physics
Open Access
EGU

Measurement report: Brown carbon aerosol in polluted urban air of the North China Plain – day–night differences in the chromophores and optical properties

Yuquan Gong[1,2], Ru-Jin Huang[1,2,3], Lu Yang[1,2], Ting Wang[1], Wei Yuan[1,2], Wei Xu[1], Wenjuan Cao[1], Yang Wang[4,5], and Yongjie Li[6]

[1]State Key Laboratory of Loess and Quaternary Geology, CAS Center for Excellence in Quaternary Science and Global Change, Institute of Earth Environment, Chinese Academy of Sciences, 710061 Xi'an, China
[2]University of Chinese Academy of Sciences, Beijing 100049, China
[3]Institute of Global Environmental Change, Xi'an Jiaotong University, Xi'an 710049, China
[4]School of Geographical Sciences, Hebei Normal University, Shijiazhuang, China
[5]State Key Joint Laboratory of Environmental Simulation and Pollution Control, Beijing, China
[6]Department of Civil and Environmental Engineering, Faculty of Science and Technology, University of Macau, Taipa, Macau SAR 999078, China

Correspondence: Ru-Jin Huang (rujin.huang@ieecas.cn)

Received: 3 January 2023 – Discussion started: 2 March 2023
Revised: 21 July 2023 – Accepted: 16 October 2023 – Published: 14 December 2023

Abstract. Brown carbon (BrC) aerosol is light-absorbing organic carbon that affects radiative forcing and atmospheric photochemistry. The BrC chromophoric composition and its linkage to optical properties at the molecular level, however, are still not well characterized. In this study, we investigate the day–night differences in the chromophoric composition (38 species) and optical properties of water-soluble and water-insoluble BrC fractions (WS-BrC and WIS-BrC) in aerosol samples collected in Shijiazhuang, one of the most polluted cities in China. We found that the light absorption contribution of WS-BrC to total BrC at 365 nm was higher during the day (62 ± 8 %) than during the night (47 ± 26 %), which is in line with the difference in chromophoric polarity between daytime (more polar nitrated aromatics) and nighttime (more less-polar polycyclic aromatic hydrocarbons, PAHs). The high polarity and water solubility of BrC in the daytime suggests the enhanced contribution of secondary formation to BrC during the day. There was a decrease in the mass absorption efficiency of BrC from nighttime to daytime (2.88 ± 0.24 vs. 2.58 ± 0.14 for WS-BrC and 1.43 ± 0.83 vs. $1.02 \pm 0.49\ m^2\ g\ C^{-1}$ for WIS-BrC, respectively). Large polycyclic aromatic hydrocarbons (PAHs) with four- to six-ring PAHs and nitrophenols contributed to 76.7 % of the total light absorption between 300–420 nm at nighttime, while nitrocatechols and two- to three-ring oxygenated PAHs accounted for 52.6 % of the total light absorption during the day. The total mass concentrations of the identified chromophores showed larger day–night difference during the low-pollution period (day-to-night ratio of 4.3) than during the high-pollution period (day-to-night ratio of 1.8). The large day–night difference in BrC composition and absorption, therefore, should be considered when estimating the sources, atmospheric processes, and impacts of BrC.

Published by Copernicus Publications on behalf of the European Geosciences Union.

1 Introduction

Light-absorbing organic carbon aerosols, also termed brown carbon (BrC) aerosol, are ubiquitous in the atmosphere (Iinuma et al., 2010; Yuan et al., 2016; Huang et al., 2021). Growing evidence has shown that BrC can reduce atmospheric visibility, affect atmospheric photochemistry, and change the regional and global radiation balance (Kirchstetter et al., 2004; Laskin et al., 2015; Hammer et al., 2016). Besides, some components in BrC, such as polycyclic aromatic hydrocarbons (PAHs), are highly toxic and carcinogenic, which can adversely impact human health (Alcanzare, 2006; Zhang et al., 2009; Huang et al., 2014). The extent of these effects is closely related to the optical properties and chemical composition of BrC, which are still not well understood.

BrC is often classified into water-soluble (WS-BrC) and water-insoluble (WIS-BrC) fractions because these two fractions are largely different in chemical composition and light absorption. For example, abundant nitrophenols were detected in WS-BrC, while polycyclic aromatic hydrocarbons (PAHs) were the main component of WIS-BrC (Huang et al., 2018, 2020). The difference in BrC chemical composition is associated with the emission sources. For example, methyl nitrocatechols are specific to biomass burning, while PAHs are mainly emitted by fossil fuel combustion (Kitanovski et al., 2012; Dat and Chang, 2017). Atmospheric oxidation can further complicate the BrC chromophores dynamically, leading to light-absorbing enhancement or bleaching. For example, Li et al. (2020) reported that the mass absorption efficiency (MAE) of some nitroaromatic compounds (e.g., nitrocatechols) from biomass burning can be enhanced by about 2–3 times by oxidation to generate secondary chromophores. Yet, prolonged photo-oxidation reactions (exposure to sunlight for few hours) of these nitroaromatic can generate small fragment molecules (e.g., malonic acid, glyoxylic acid) and rapidly reduce the particle absorption (Hems and Abbatt, 2018; Y. Wang et al., 2019; Li et al., 2020). The complexity in composition and sources, as well as the dynamics in their atmospheric processing, limits our understanding in BrC chromophores and their links to light absorption.

In recent years, a growing number of studies have investigated the chromophore composition of BrC and found that nitrophenols, low-ring acids/alcohols, PAHs, and carbonyl oxygenated PAHs (OPAHs) were the major chromophores in BrC (Teich et al., 2017; Yuan et al., 2020; Huang et al., 2020). Some chromophores in BrC can be generated from both primary emission and secondary formation. For example, 4-nitrophenol and 4-nitrocatechol can be emitted directly from biomass burning and can also be generated through photo-oxidation reactions (Kitanovski et al., 2012; Yuan et al., 2020). The differences in emission sources or atmospheric oxidation conditions have a significant effect on the chemical composition of BrC chromophores. Previous studies mainly focused on seasonal variations of BrC chromophores (Wang et al., 2018; Kasthuriarachchi et al., 2020; Yuan et al., 2021) and the diurnal variation of WS-BrC in fluorescence and inorganic fractions (Deng et al., 2022; Zhan et al., 2022; Li et al., 2021); however, the research of BrC chemical composition on day–night differences is scarce. In this study, the optical properties and chemical composition of WS-BrC and WIS-BrC in both daytime and nighttime $PM_{2.5}$ samples collected in Shijiazhuang, one of the most heavily polluted cities in the Beijing–Tianjin–Hebei region, were analyzed using a high-performance liquid chromatography (HPLC) system equipped with a photodiode array (PDA) detector and a high-resolution Orbitrap mass spectrometer (HRMS). The $PM_{2.5}$ samples were collected in Shijiazhuang, one of the most heavily polluted cities in the Beijing–Tianjin–Hebei region. Besides, the relationship between the concentration and light-absorbing contributions of the BrC subgroups was analyzed. The object of this study is to investigate the day–night differences in the optical properties and chromophore composition of BrC and to explore the effect of primary emissions and atmospheric processes on the light absorption and chemical composition of BrC.

2 Experimental

2.1 Sample collection

Day and night $PM_{2.5}$ samples were collected on the quartz-fiber filters (8 × 10 in., Whatman, QM-A; filters prebaked at 750 °C, over 3 h) through a high-volume air sampler (Hi-Vol $PM_{2.5}$ sampler, Tisch, velocity of flow $\sim 1.03\,m^3\,min^{-1}$, Cleveland, OH) from 17 January to 13 February 2014. Daytime samples were collected from 08:30 to 18:30 ($\sim$ 10 h), and nighttime samples are collected from 18:30 to the next day at 08:30 ($\sim$ 14 h). After collection, the samples were stored in a freezer (−20 °C) until analysis. The sampling site was located on the rooftop of a building ($\sim$ 15 m above ground) in the Institute of Genetics and Developmental Biology, Chinese Academy of Sciences (38.2° N, 114.3° E), which is surrounded by a residential–business mixed zone.

2.2 Light absorption measurement

A portion filter (about $0.526\,cm^2$ punch) was taken from collected samples and sonicated for 30 min in 10 mL of ultrapure water (>18.2 MΩ) or methanol (J. T. Baker, HPLC grade), and then the extracts WS-BrC and methanol-soluble BrC (MS-BrC) were obtained. The extracts were filtered with a 0.45 µm polyvinylidene fluoride (PVDF; water-soluble) or polytetrafluoroethylene (PTFE; water-insoluble) pore syringe filter to remove insoluble substances. The light absorption spectra of the filtrate were tested using a UV–VIS spectrophotometer (Ocean Optics) over the range from 250 to 700 nm, equipped with a liquid waveguide capillary cell (LWCC-3100, World Precision Instruments, Sarasota, FL, USA), following the method of Hecobian et al. (2010). To en-

sure reliable absorbance measurements (absorbance between 0.2 and 0.8 at 300 nm in this study), the filtrate was diluted with appropriate folds before absorption spectra measurements. In this study, the light absorption of WIS-BrC is obtained from MS-BrC minus WS-BrC. As shown in Fig. S1, the summed absorbance of WS-BrC and WIS-BrC is very close to the absorbance of MS-BrC (difference less than 5 %). Therefore, the interferences of solvent and pH on the measurement of WIS-BrC should be very limited. The pH of the water extracts was not adjusted because highly diluted water extracts were used to measure the light absorption, and little change in pH was observed for water extracts of different samples. The light absorption coefficient (Abs) and absorption data were calculated following the equation

$$\mathrm{Abs}_\lambda = (A_\lambda - A_{700})\frac{V_l}{V_b \times l} \times \ln(10), \quad (1)$$

where Abs_λ (Mm^{-1}) represents the sample absorption coefficient at a wavelength of λ, A_λ is the absorbance recorded (random wavelength), and A_{700} is for explaining baseline drift as the reference during data analysis. To account for baseline drift that may occur during analysis, absorption at all wavelengths below 700 nm is referenced to that at 700 nm, where there is no absorption for BrC extracts. V_l (mL) is the total volume of solvent (water or methanol) used to extract the quartz-fiber filters; V_b (m^3) is the volume of the air sampled through the filter punch; l (0.94 m) is the optical path length of the UV–VIS spectrophotometer; and ln (10) is the absorption coefficient with base e, which is the natural logarithm using the logarithm conversion with the base 10.

The mass absorption efficiency (MAE) of the filter extracts at a wavelength of λ can be defined as

$$\mathrm{MAE}_\lambda = \mathrm{Abs}_\lambda / C_{\mathrm{OM}}, \quad (2)$$

where C_{OM}($\mu\mathrm{g\,m}^{-3}$) stands for the concentration of water-soluble organic carbon (WSOC) or methanol-soluble organic carbon (MSOC). The concentrations of WSOC were measured with a total-organic-carbon–total-nitrogen (TOC–TN) analyzer (TOC-L, Shimadzu, Japan). The concentration of organic carbon (OC) was measured by a thermal–optical carbon analyzer (DRI, model 2001) with the IMPROVE A protocol (Chow et al., 2011). Note that MSOC is usually replaced with OC because previous studies have shown that methanol has a high extraction efficiency ($\sim$ 90 %) for OC. But it is difficult to completely extract the OC by methanol (Chen and Bond, 2010; Cheng et al., 2016; Xie et al., 2019). Here, water-insoluble organic carbon (WISOC) is obtained from MSOC minus WSOC.

The wavelength dependence for light absorption by chromophores in solution can be characterized by a power law equation:

$$\mathrm{Abs}_\lambda = K \cdot \lambda^{-\mathrm{AAE}}, \quad (3)$$

where K is the fitting parameter of the extracts which is constant related to the chromophoric concentration, and AAE is known as the absorption Ångström exponent, which depends on the types of chromophores in the solution. In this study, AAE was calculated by linear regression of $\log_{10}\mathrm{Abs}_\lambda$ versus $\log_{10}\lambda$ at 300–400 nm.

The MAE values of authentic standards including nitrophenols, PAHs, and OPAHs ($\mathrm{MAE}_{\mathrm{S},\lambda}$) at a wavelength of λ were calculated by the following equation (Laskin et al., 2015):

$$\mathrm{MAE}_{\mathrm{S},\lambda} = \frac{A_\lambda - A_{700}}{l \times C}\ln(10), \quad (4)$$

where C ($\mu\mathrm{g\,mL}^{-1}$) is the concentration of the standards in the extracts.

2.3 BrC chemical composition analysis

The main chromophores in WS-BrC and WIS-BrC were identified by the HPLC–PDA–HRMS platform (Thermo Electron, Inc.), and the details are presented in our previous study (Huang et al., 2020). Firstly, the filter samples ($3.5 \sim 48.3\ \mathrm{cm}^2$) were ultrasonically extracted with 6 mL of the ultrapure water for 30 min and repeated two times. The extracts were filtered through a PVDF filter (0.45 µm) to remove insoluble materials. Then the solution was subjected to a solid phase extraction (SPE) cartridge (Oasis HLB, USA) to remove water-soluble inorganic salt ions. On the other hand, the residual filters were dried and the WIS-BrC fractions were further extracted two times with 6 mL of methanol for 30 min to extract the WIS-BrC fractions. Afterward, the extracts of WS-BrC and WIS-BrC chromophores were dried with a gentle stream of nitrogen and then redissolved in 150 µL of ultrapure water and methanol.

The BrC factions were analyzed by an HPLC–PDA–HRMS platform (including the Dionex UltiMate system and the high-resolution Q Exactive Plus hybrid quadrupole–Orbitrap mass spectrometer). Here, the extracts were loaded onto an Accucore RP-MS column (Thermo Scientific) by the binary solvent with an aqueous solution containing 0.1 % formic acid and a methanol solution containing 0.1 % formic acid as mobile phases L_1 and L_2, eluting at a flow rate of $0.3\ \mathrm{mL\,min}^{-1}$. The process of gradient elution was set as follows: the concentration of L_2 was held at 15 % at the beginning and then linearly increased to 30 % from 0 to 15 min, linearly increased to 90 % from 15 to 45 min, held at 90 % from 45 to 50 min, and then decreased to 15 % from 50 to 52 min and held there for 60 min. The spectrometer was equipped with an electrospray ionization (ESI) source and details about the operation parameters are similar to those of previous studies (Liu et al., 2016; Huang et al., 2020). Briefly, the mass spectra of different BrC fractions in Shijiazhuang were acquired in both negative (ESI (−)) and positive (ESI (+)) modes in the mass range between m/z 100 and 800. Strongly polar aromatic hydrocarbons like nitrophenol and carboxylic acid are preferentially ionized in ESI (–) mode (Lin et al., 2017). OPAHs and nitrogen heterocyclic

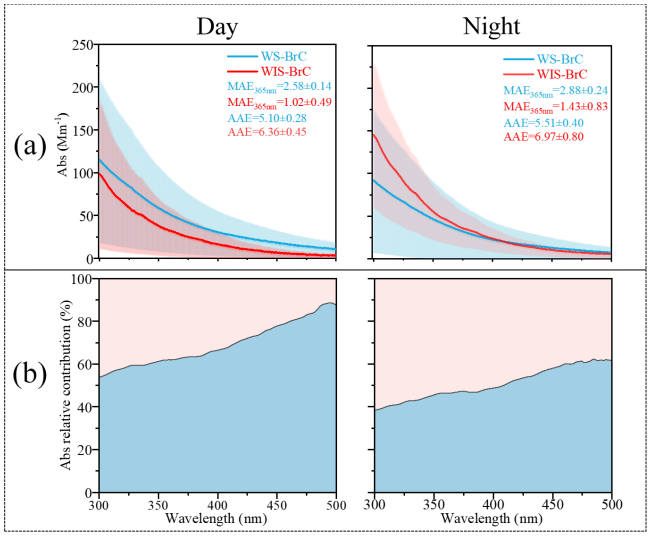

Figure 1. **(a)** Day–night absorption spectra (Abs, in the wavelength range of 300–500 nm), mass absorption efficiency (MAE, determined at 365 nm), and absorption Ångström exponent (AAE, calculated between 300 and 400 nm) of water-soluble/insoluble BrC (WS-/WIS-BrC) in Shijiazhuang. **(b)** Light-absorbing proportion of WS-BrC and WIS-BrC between 300 and 500 nm.

PAHs were quantified in ESI (+) mode, while PAHs were detected by PDA spectroscopic analysis due to their super low ionization efficiency in ESI. The absorption spectra of chromophores were measured by a PDA detector in the wavelength range of 190–700 nm. The results of this study were corrected using a blank.

The elemental composition of individual chromatographic peaks was assigned with the molecular formula calculator in Xcalibur 4.0 software using a mass tolerance of ±3 ppm, and the maximum numbers of atoms for the formula calculator were set as 30 ^{12}C, 60 ^{1}H, 15 ^{16}O, 3 ^{14}N, 1 ^{32}S, and 1 ^{23}Na. To eliminate the chemically unreasonable formulas, the identified formulas were constrained by setting $0.3 \le H/C \le 3.0$, $0.0 \le O/C \le 3.0$, $0.0 \le N/C \le 0.5$, and $0.0 \le S/C \le 0.2$ in ESI mode and $0.3 \le H/C \le 3.0$, $0.0 \le O/C \le 3.0$, $0.0 \le N/C \le 1.3$, and $0.0 \le S/C \le 0.8$ in ESI+ mode, as suggested in a previous study (Lin et al., 2012). Further, the calculated neutral molecular formulas that did not fit the nitrogen rule were excluded. In total, 20 WS-BrC chromophores (two quinolines, four two- to three-ring OPAHs, four nitrocatechols, six nitrophenols, and four aromatic alcohols and acids) and 18 WIS-BrC chromophores (three four-ring OPAHs and 15 PAHs) were identified, and their concentrations were quantified with authentic standards (28 species) or surrogates (10 species) (see Table S1). Therein, the WS-BrC chromophores, benzanthrone (21#) and benzo[b]fluoren-11-one (22#), were quantified by mass spectrometry analysis in either negative or positive ESI mode, while the rest of WIS-BrC chromophores were quantified by PDA spectroscopic analysis due to their super low ionization efficiency in ESI (see Table S1).

3 Results and discussion

3.1 Optical properties of BrC during the day and night

Figure 1a shows the average absorption spectra of WS-BrC and WIS-BrC at the wavelength range between 300 and 500 nm during the day and the night. It can be seen that the light absorption of both WS-BrC and WIS-BrC sharply increased toward the short wavelength. The average absorbance of WS-BrC is $46.04 \pm 35.92\ Mm^{-1}$ (at 365 nm) during the day, which is higher than at night ($35.68 \pm 35.50\ Mm^{-1}$). However, the light absorption of WIS-BrC at 365 nm is much lower during the night ($27.90 \pm 24.80\ Mm^{-1}$) than during the day ($40.89 \pm 23.42\ Mm^{-1}$). The day–night differences of light absorption of WS-BrC and WIS-BrC indicate the difference in water solubility and polarity of the chromophores. The average AAE of WS-BrC ($AAE_{WS\text{-}BrC}$) and WIS-BrC ($AAE_{WIS\text{-}BrC}$) during the day are 5.10 ± 0.28 and 6.36 ± 0.45, respectively, which are lower than those at night (5.51 ± 0.40 and 6.97 ± 0.80, respectively). Note that during both the day and night the $AAE_{WS\text{-}BrC}$ is lower than $AAE_{WIS\text{-}BrC}$, which is different from findings in previous studies (see Table S2). For example, Huang et al. (2020) found that the $AAE_{WS\text{-}BrC}$ was higher (8.2 ± 1.0 and 8.2 ± 1.0 in Beijing and Xi'an, respectively) than that of $AAE_{WIS\text{-}BrC}$ (5.7 ± 0.2 and 5.4 ± 0.2 in Beijing and Xi'an, respectively). Besides, MAE_{365} values of WS-BrC (2.88 ± 0.24 and $2.58 \pm 0.14\ m^2\ g\ C^{-1}$) are 2.0 and 2.5 times those of WIS-BrC (1.43 ± 0.83 and $1.02 \pm 0.49\ m^2\ g\ C^{-1}$) during the day and night, respectively. For example, the MAE_{365} values of WS-BrC (1.22 ± 0.11 and $1.00 \pm 0.18\ m^2\ g\ C^{-1}$) are 0.7 and 0.5 times those of WIS-BrC (1.66 ± 0.48 and $1.82 \pm 1.06\ m^2\ g\ C^{-1}$) in winter for Beijing (Cheng et al., 2016) and Xi' an (Li et al., 2020), respectively. This result indicates that the chemical composition of BrC in the most polluted city, Shijiazhuang, is different from other urban areas on primary sources and secondary aging process. However, both WS-BrC and WIS-BrC have higher MAE_{365} and average AAE values during the day than the night. This suggests that the day–night differences of AAE and MAE_{365} of BrC fractions are likely associated with the different primary emissions and atmospheric aging processes (Cheng et al., 2016; Q. Wang et al., 2019; Wang et al., 2020). For example, the AAE and MAE_{365} of BrC emitted from biomass burning ($AAE \sim 7.31$ and $MAE_{365} \sim 1.01\ m^2\ g\ C^{-1}$, respectively) (Siemens et al., 2022) showed large differences compared to that from vehicle emissions ($AAE \sim 10.5$ and $MAE_{365} \sim 0.32\ m^2\ g\ C^{-1}$) (Xue et al., 2018). Besides, photochemical oxidation of fresh BrC from coal combustion resulted in considerable changes in AAE and MAE_{365}; e.g., the AAE and MAE_{365} of fresh coal combustion emission are 7.2 and $0.84 \pm 0.54\ m^2\ g\ C^{-1}$,

which is much higher than those in aged samples (6.4 and $0.14 \pm 0.08\ m^2\ g\ C^{-1}$, respectively) (Ni et al., 2021).

Figure 1b shows the light absorption contributions of WS-BrC and WIS-BrC to total BrC over the wavelength range of 300–500 nm. It is obvious that the absorption contribution of WS-BrC is increased from 53.8 % at 300 nm to 87.4 % at 500 nm during the day and from 38.4 % to 61.5 % during the night. The higher absorption contributions of WS-BrC at longer wavelengths during the day compared to that of the night may be related to photo-oxidation reaction in the daytime (Y. Wang et al., 2019; Chen et al., 2021). The absorption contribution of WS-BrC accounts for 62 ± 8 % of the total BrC absorption at 365 nm during the day but only 47 ± 8 % during the night. The large difference in BrC light absorption between samples from the day and those from the night observed in this study is comparable with previous studies (Shen et al., 2019; Li et al., 2020) and indicates the significant day–night difference in chemical composition.

3.2 Composition and absorption contribution of BrC during the day and night

In total, 38 major chromophores were quantified in WS-BrC and WIS-BrC with HPLC–PDA–HRMS analysis, and the concentrations of these chromophores are shown in Table S3. According to the characteristics of the molecular structures and absorption spectra, these chromophores are divided into 10 subgroups, including two quinolines, four nitrocatechols, six nitrophenols, four aromatic alcohols/acids, four two- to three-ring OPAHs, three four-ring OPAHs, two three-ring PAHs, four four-ring PAHs, five five-ring PAHs, and four six-ring PAHs. Detailed information about these chromophores is listed in Table S4. Figure 2 shows the chemical composition of the identified BrC components during the day and night. The total concentration of these chromophores during the day ($169.8\ ng\ m^{-3}$) is similar to that at night ($171.8\ ng\ m^{-3}$), and the chemical composition of the BrC subgroups is clearly different between the day and night. For example, nitrocatechols, aromatic alcohols/acids, and two- to three-ring OPAHs are the major contributors to the total mass concentration of identified BrC chromophores during the day (accounting for 23.3 %, 22.3 %, and 16.6 %, respectively). These BrC chromophores, however, are the minor components during the night (accounting for 12.1 %, 15.6 %, and 6.9 %, respectively). This result indicates the enhanced formation of these chromophores during the day. On the contrary, the relative contributions of nitrophenols and four- to six-ring PAHs are much lower during the day (15.3 % and 15.2 %, respectively) than those during the night (35.8 % and 24.0 %, respectively). During the night, 4-nitrophenol (4NP) contributes 24.4 % of the total concentration, followed by 2-methyl-4-nitrophenol, fluoranthene, and chrysene (2M4NP 4.7 %, FLU 4.6 %, CHR 4.6 %, respectively). The higher contributions of nitrophenols and four- to six-ring PAHs at night are likely caused by enhanced primary emissions (Lin et al., 2020; Chen et al., 2021). Our previous study has found that the emitted organic aerosols from coal combustion had a clear increase at midnight in Shijiazhuang (Huang et al., 2019; Lin et al., 2020). Thus, the large contribution of nitrophenols and four- to six-ring PAHs to total mass concentration at night may be impacted by emissions from the coal combustion.

To investigate the source of the BrC chromophores, the mass concentrations (these concentrations of chromophores are OC normalized) of the day and night were compared. The day-to-night ratios of identified BrC compounds in mass concentrations are shown in Fig. 3. It can be seen that the average day-to-night ratios of WS-BrC chromophores are 4.87 for quinolines, 3.49 for two- to three-ring OPAHs, 3.47 for nitrocatechols, 0.48 for nitrophenols, and 2.53 for aromatic alcohols/acids, respectively. Previous studies have found that quinolines are important products of fossil fuel combustion and were used as tracers of the vehicular exhaust (Banerjee and Zare, 2015; Xue et al., 2018; Lyu et al., 2019). Thus, the higher day-to-night ratio of quinolines may be due to increased primary emissions from vehicles during the day. Nitrophenols and vanillin are typical biomass burning tracers for atmospheric aerosols (Harrison et al., 2005; Scaramboni et al., 2015; Huang et al., 2021). Previous studies have identified secondary formation as an important source of phthalic acid (PA) and methyl-nitrocatechols (Chow et al., 2015; Zhang and Hatakeyama, 2016; Liu et al., 2017). In this study, vanillin, phthalic acid, and three methyl-nitrocatechols (including 4M5NC, 3M6NC, and 3M5NC) isomers have high day-to-night ratios (4.16, 3.75, and 3.28, respectively). The high day-to-night ratios of these BrC chromophores suggest that biomass burning and secondary formation likely play important roles in the daytime source of BrC.

The average day-to-night ratio (~ 0.48) of nitrophenols is smaller than 1, and this result is similar to previous studies (Yuan et al., 2016; Schnitzler and Abbatt, 2018). Although both nitrophenols and nitrocatechols can be emitted from biomass burning, they show largely different day–night variation patterns. The higher concentrations of nitrocatechols during daytime indicate enhanced secondary formation, which is similar to the results observed in urban Beijing (Cheng et al., 2021). In addition, previous studies found that emissions from residential coal-fired heating are significant sources of nitrophenols (Wang et al., 2018; Lu et al., 2019). The higher concentrations of nitrophenols during nighttime, however, suggest that they are mainly emitted from primary emission sources such as residential heating during winter in North China. Compared with the WS-BrC chromophores (the day-to-night ratio >2.53), the day-to-night ratios of the WIS-BrC chromophores approach or are below 1, with average ratios of 1.46 for three-ring PAHs, 1.34 for four-ring OPAHs, 0.74 for four-ring PAHs, 0.91 for five-ring PAHs, and 0.79 for six-ring PAHs. A number of studies showed that coal combustion was the dominant source of PAHs (Wang et al., 2018; Xie et al., 2019; Yuan et al., 2020). Thus, the lo-

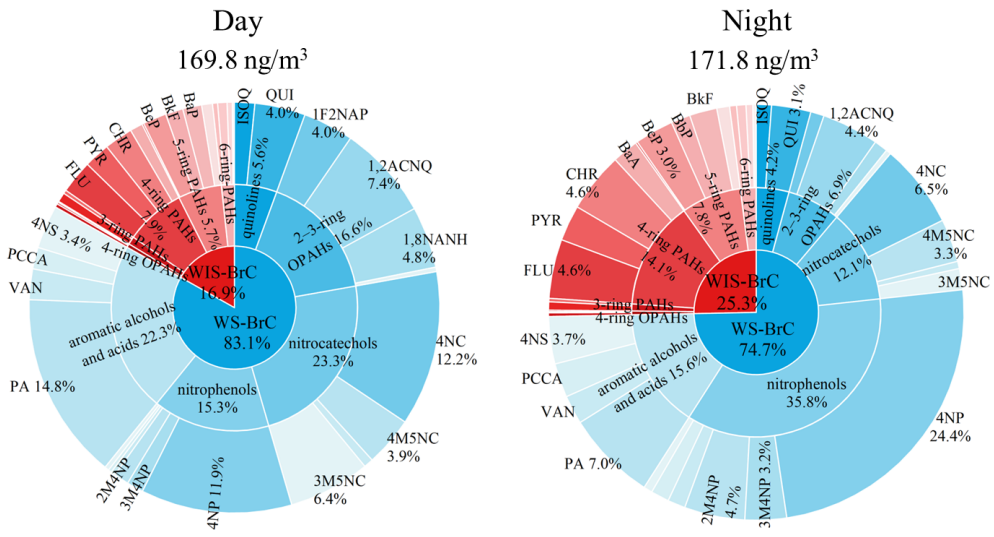

Figure 2. Mass fraction of the identified BrC chromophores during the day and night (details of the identified BrC chromophores are shown in Table S1).

cal emissions may be responsible for the majority of four- to six-ring PAHs during the night.

Figure S2 shows the light absorption contributions of the BrC subgroups to total BrC subgroups in the wavelength range between 300 and 420 nm (the absorptions above 420 nm are too low to exactly estimate the contributions), exhibiting large day–night differences. For example, quinolines show evident absorption below 340 nm (3.6 % at 310 nm during the day) but negligible contribution above 360 nm. Nitrophenols exhibit a maximum contribution at about 350 nm, while nitrocatechols show higher absorption in the wavelength range from 360 to 400 nm. For PAHs, the absorption maxima shift to a longer wavelength with the increase in the aromatic rings (e.g., 320 nm for four-ring PAHs and 400 nm for six-ring PAHs). Overall, the combined light absorption contributions of nitrophenols, nitrocatechols, and PAHs are 86.5 % and 80.1 % (averaged between 300 and 420 nm) at night and during the day, respectively. This result is similar to previous studies in which PAHs and nitroaromatic compounds were identified as the major chromophores (Huang et al., 2020; Yuan et al., 2020).

The light absorption contribution of these BrC subgroups exhibits obvious day–night differences. For example, the absorption contribution of two- to three-ring OPAHs and nitrocatechols at 365 nm increased by ~ 2.0 and ~ 3.5 times during the day compared to that during the night (see Fig. S3). This result differs from previous studies (Kampf et al., 2012; Gao et al., 2022), which indicated that light absorption of BrC compounds were enhanced after exposure to photooxidation. On the other hand, the absorption contributions of nitrophenols and four- to six-ring PAHs at 365 nm are ~ 1.6 times and ~ 2.2 times higher at night than during the day, respectively. The day–night difference of light absorption of nitrophenols is comparable with previous studies (Harrison et al., 2005; Wang et al., 2020). High absorbance of nitrophenols at night is closely related to their higher mass fraction at night. The absorption characteristics of four- to six-ring PAHs are significantly different from the nitrophenols, and their absorption per unit mass is larger than that of nitrophenols. The much higher per-unit-mass absorbance of PAHs than the low-ring aromatic hydrocarbons (e.g., aromatic alcohols/acids) is due to their strongly conjugated systems. It is worth noting that the absorption contributions of some BrC compounds (including quinolines, aromatic alcohols/acids, four-ring OPAHs, three-ring PAHs four subgroups) are much lower than those of the above-mentioned BrC compounds because of their lower mass concentration or light absorption coefficient.

3.3 Comparisons between the low- and high-pollution period

The relative contributions of day–night subgroups of BrC chromophores in light absorption and mass concentration were further investigated for different pollution levels. The sampling campaign was classified into a low-pollution period ($PM_{2.5} < 150\,\mu g\,m^{-3}$) and a high-pollution period ($PM_{2.5} > 250\,\mu g\,m^{-3}$). Figure 4a shows the mass fractional contributions of the identified subgroups during these periods, which show an evidently different composition during day and night. For example, the mass fraction of quinolines during the day (~ 24.1 %) is much higher than during the night (3.4 %) in the low-pollution period, which may be related to increased vehicle emissions during the day (Rogge et al., 1993; Lyu et al., 2019). Moreover, during the low-pollution period, with good atmospheric dispersion conditions during the day, the fractional concentration of BrC is only $56.9\,ng\,m^{-3}$, which is much lower than the nights and

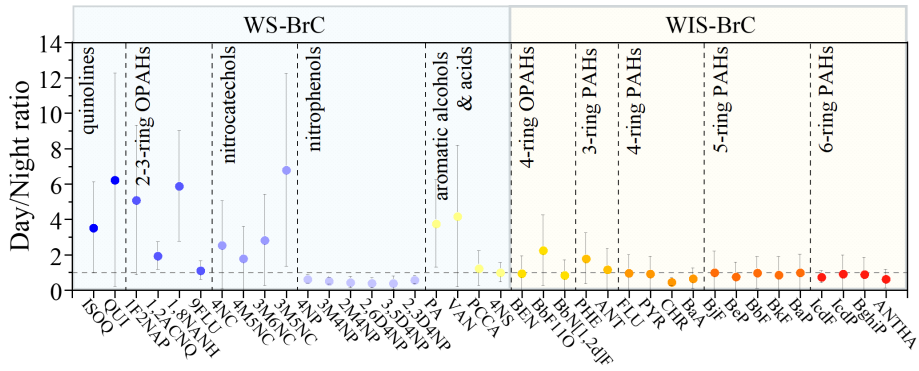

Figure 3. Day-to-night ratios of the concentrations of different BrC chromophores.

high-pollution periods. In the high-pollution period, however, the mass concentration of quinolines is much lower than other BrC chromophores, and there is no evident difference between day and night. The mass fraction of aromatic alcohols/acids during the day (35.4 %) is much higher than during the night (12.0 %) in the low-pollution period. For the high-pollution period, the mass fraction of aromatic alcohols/acids shows little difference between the day and night. However, their mass concentration during the day (55.5 ng m^{-3}) is higher than that during the night (31.9 ng m^{-3}). Therein, the mass concentration of phthalic acid (a tracer from photochemical oxidation) contributes more than 60 % to the aromatic alcohols/acids during the day for the low- and high-pollution period (Zhang and Hatakeyama, 2016). This evidence may suggest that there is stronger photo-chemical oxidation for aromatic alcohols/acids during the day, especially in the low-pollution period.

The mass fractional contribution of nitrocatechols is lower during the day than the night in the low-pollution period, while there is obvious secondary formation during the day for the high-pollution period. This likely suggests that the daytime conditions of the high-pollution period are inductive for the generation of nitrocatechols. The mass fractional contribution of PAHs during the day is much lower than the night in the low-pollution period. At night, residential coal heating is an important source of PAHs, and therefore the daytime contributions of PAHs are much lower than the nighttime ones (Wang et al., 2017; Ni et al., 2021), while there is no day–night difference for PAHs in the high-pollution period, which is related to the stable sources and stagnant weather conditions (Huang et al., 2019; Lin et al., 2020). It is noteworthy that the mass contributions of the nitrophenols (nighttime is 2–3 times more than daytime) and two- to three-ring OPAHs (daytime is ∼ 2 times more than nighttime) are opposite between the day and night. This demonstrates that they have stable sources compared to other BrC subgroups even during the low-pollution period and high-pollution period. The higher mass fractional contribution of two- to three-ring OPAHs during the day is related to photochemical oxidation. Nitrophenols exhibit a higher mass fractional contribution during the night than the day, indicating a significant contribution from primary emissions (Lu et al., 2019; Lin et al., 2020). Besides, previous investigations have shown that NO_x concentrations and relative humidity are higher at night in Shijiazhuang, which may have accelerated the formation of nitrophenols in the dark (Yuan et al., 2016; Huang et al., 2019). This result exhibits a clear day–night difference during the low-pollution period compared to the high-pollution period, which indicates that the low-pollution period is easily influenced by the external environment (e.g., solar radiation and wind speed).

The day–night light absorption contribution of WS-BrC and WIS-BrC chromophores in different pollution periods is shown in Fig. 4b. For the low-pollution period, the light absorption contribution of the 10 BrC subgroups shows a large difference during the day and night. Therein, the WS-BrC chromophores (e.g., quinolines, nitrophenols, and nitrocatechols) are the main contributor (accounting for ∼ 75 % at 365 nm) of total identified BrC during the day. While, the WIS-BrC chromophores (e.g., four- to six-ring PAHs) become an abundance contributor (accounting for ∼ 65 % at 365 nm) during the night. There is an obvious day–night difference in light absorption in the low-pollution period, which is consistent with the difference in their mass concentration contribution. Different from the low-pollution period, the light absorption contribution of the total WS-BrC and WIS-BrC chromophores showed no significant day–night differences during the high-pollution period. However, the absorption contributions of subgroups in WS-BrC chromophores have a significant day–night difference (e.g., nitrocatechol and nitrophenols) during the high-pollution period, which is due to the changes in the mass contributions. WS-BrC chromophores have stronger light absorption during the day and night compared to the WIS-BrC chromophores during the high-pollution period. Specifically, the absorption contribution of nitrocatechols and nitrophenols combined accounts for 66.1 % during the day and 60.7 % at night at 365 nm, respectively, which depends on the different emission sources

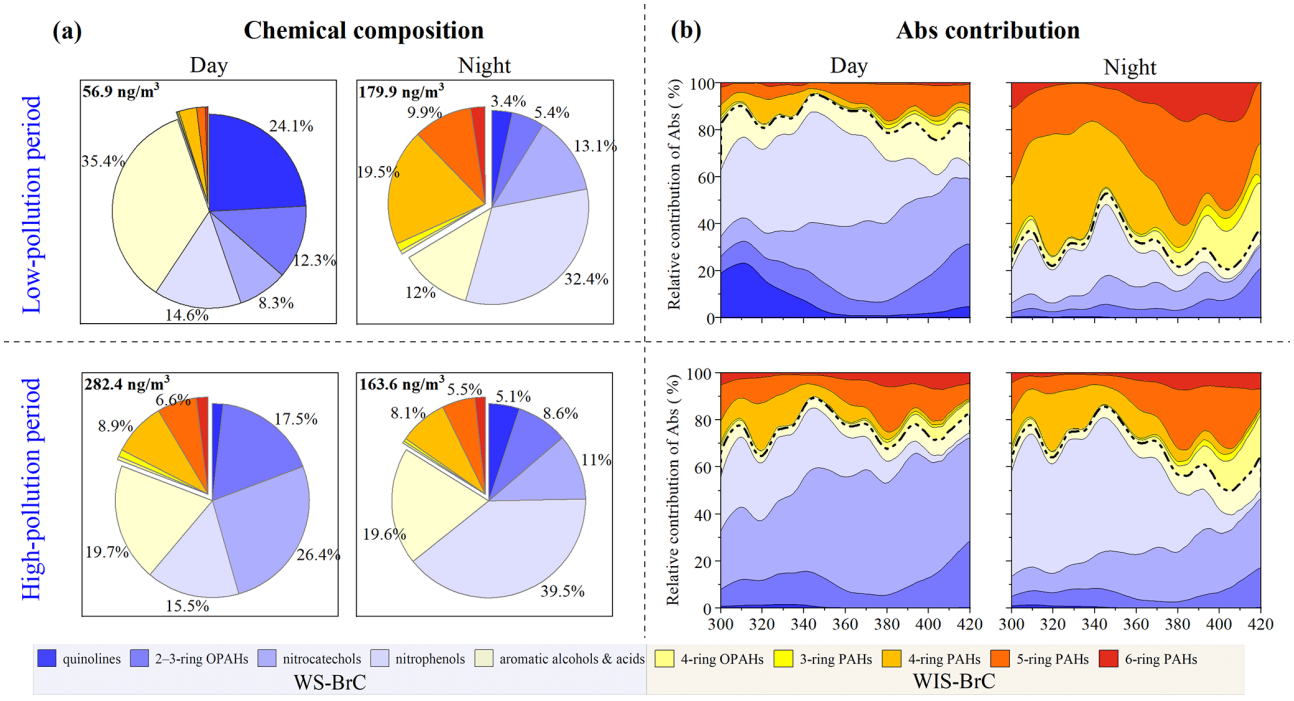

Figure 4. Day–night fractional contributions of mass concentrations **(a)** and light absorption **(b)** of the 10 BrC subgroups in the low-pollution period and high-pollution period. Here the BrC chromophore is the main chromophore substance that has been identified. In panel **(b)** WS-BrC is below the dotted line and WIS-BrC is above the dotted line.

or formation mechanisms between the day and night. Our results show a significant day–night difference in mass contributions and absorption contributions of BrC components at different pollution levels. This suggests that the variation of BrC chromophores in different pollution periods may be caused by different sources and weather conditions.

4 Conclusions

In general, our study shows the large day–night differences in optical properties and chemical composition of the bulk BrC in the urban atmosphere. Therein, WS-BrC is the main light-absorbing contributors during the day, while WIS-BrC is the main light-absorbing compound at night. The polar WS-BrC has higher MAE_{365} values compared to the less-polar WIS-BrC, mainly due to the different conjugate systems and functional groups in the two fractions. Different types of the identified BrC chromophores exhibit unique characteristics of day–night differences, reflecting their particular sources and formation pathways. For example, nitrocatechols and two- to three-ring OPAHs are important contributors to mass concentration and light absorption during the day, while four- to six-ring PAHs and nitrophenols become the significant contributors at night.

Day–night differences of BrC chromophores are associated with different sources during the day (mainly secondary formation and vehicle emission) and night (mainly emissions from residential heating) as well as the dynamic development of planetary boundary layer height. Moreover, these day–night differences are largely affected by the air pollution level, which determines the concentrations of BrC precursors (e.g., aromatic hydrocarbon and phenols) and oxidants (e.g., NO_x, $NO_3^{\bullet}$, and OH), as well as meteorological conditions (e.g., solar irradiation and RH) (Liu et al., 2012; Laskin et al., 2015; Wang et al., 2019). For example, our results found that the day–night difference of BrC fractions is more pronounced in chemical composition and light absorption during the low-pollution period than the high-pollution period. These factors may show different effects on the formation and photobleaching of different types of the identified chromophores. However, our current understanding of the formation mechanisms of and influencing factors on these identified chromophores is still incomplete (Huang et al., 2018; Yuan et al., 2020). Therefore, a combination of more laboratory and field studies is needed to (1) make a comprehensive characterization of the chromophore composition BrC in ambient aerosol and (2) explore thoroughly the formation mechanisms of different types of BrC chromophore. This will significantly enhance our understanding of atmospheric BrC formation mechanisms and therefore improve the accuracy of the atmospheric effects of BrC in air quality and climate models.

Data availability. Detailed data can be obtained from https://doi.org/10.5281/zenodo.7690230 (Gong, 2023).

Supplement. The supplement related to this article is available online at: https://doi.org/10.5194/acp-23-15197-2023-supplement.

Author contributions. R-JH designed the study. Data analysis was done by YG and R-JH. YG and R-JH interpreted data, prepared the figures, and wrote the manuscript. LY, TW, WY, WX, WC, YW, and YL commented on and discussed the manuscript.

Competing interests. The contact author has declared that none of the authors has any competing interests.

Disclaimer. Publisher's note: Copernicus Publications remains neutral with regard to jurisdictional claims made in the text, published maps, institutional affiliations, or any other geographical representation in this paper. While Copernicus Publications makes every effort to include appropriate place names, the final responsibility lies with the authors.

Acknowledgements. We are very grateful to the National Natural Science Foundation of China (NSFC) (no. 41925015), the Strategic Priority Research Program of the Chinese Academy of Sciences (no. XDB40000000), the Key Research Program of Frontier Sciences from the Chinese Academy of Sciences (no. ZDBS-LY-DQC001), and the Cross Innovative Team fund from the State Key Laboratory of Loess and Quaternary Geology (no. SKLLQGTD1801), who supported this study.

Financial support. This work was supported by the National Natural Science Foundation of China (NSFC) under grant no. 41925015, the Strategic Priority Research Program of the Chinese Academy of Sciences (grant no. XDB40000000), the Key Research Program of Frontier Sciences from the Chinese Academy of Sciences (grant no. ZDBS-LY-DQC001), and the Cross Innovative Team fund from the State Key Laboratory of Loess and Quaternary Geology (grant no. SKLLQGTD1801).

Review statement. This paper was edited by Stefania Gilardoni and reviewed by three anonymous referees.

References

Alcanzare, R. J. C.: Polycyclic aromatic compounds in wood soot extracts from Henan, China, M.Sc. Thesis, The Department of Chemical Engineering, Louisiana State University and Agricultural and Mechanical College, Baton Rouge, LA, 132, https://doi.org/10.31390/gradschool_theses.2377, 2006.

Banerjee, S. and Zare, R. N.: Syntheses of isoquinoline and substituted quinolines in charged microdroplets, Angew. Chem., 127, 15008–15012, 2015.

Chen, L.-W. A., Chow, J. C., Wang, X., Cao, J., Mao, J., and Watson, J. G.: Brownness of Organic Aerosol over the United States: Evidence for Seasonal Biomass Burning and Photobleaching Effects, Environ. Sci. Technol., 55, 8561–8572, https://doi.org/10.1021/acs.est.0c08706, 2021.

Chen, Y. and Bond, T. C.: Light absorption by organic carbon from wood combustion, Atmos. Chem. Phys., 10, 1773–1787, https://doi.org/10.5194/acp-10-1773-2010, 2010.

Cheng, X., Chen, Q., Li, Y., Huang, G., Liu, Y., Lu, S., Zheng, Y., Qiu, W., Lu, K., Qiu, X., Bianchi, F., Yan, C., Yuan, B., Shao, M., Wang, Z., Canagaratna, M. R., Zhu, T., Wu, Y., and Zeng, L.: Secondary Production of Gaseous Nitrated Phenols in Polluted Urban Environments, Environ. Sci. Technol., 55, 4410-4419, https://doi.org/10.1021/acs.est.0c07988, 2021.

Cheng, Y., He, K. B., Du, Z. Y., Engling, G., Liu, J. M., Ma, Y. L., Zheng, M., and Weber, R. J.: The characteristics of brown carbon aerosol during winter in Beijing, Atmos. Environ., 127, 355–364, https://doi.org/10.1016/j.atmosenv.2015.12.035, 2016.

Chow, J. C., Watson, J. G., Robles, J., Wang, X., Chen, L.-W. A., Trimble, D. L., Kohl, S. D., Tropp, R. J., and Fung, K. K.: Quality assurance and quality control for thermal/optical analysis of aerosol samples for organic and elemental carbon, Anal. Bioanal. Chem., 401, 3141–3152, 2011.

Chow, K. S., Huang, X. H., and Yu, J. Z.: Quantification of nitroaromatic compounds in atmospheric fine particulate matter in Hong Kong over 3 years: field measurement evidence for secondary formation derived from biomass burning emissions, Environ. Chem., 13, 665–673, 2015.

Dat, N. D. and Chang, M. B.: Review on characteristics of PAHs in atmosphere, anthropogenic sources and control technologies, Sci. Total Environ., 609, 682–693, https://doi.org/10.1016/j.scitotenv.2017.07.204, 2017.

Deng, J., Ma, H., Wang, X., Zhong, S., Zhang, Z., Zhu, J., Fan, Y., Hu, W., Wu, L., Li, X., Ren, L., Pavuluri, C. M., Pan, X., Sun, Y., Wang, Z., Kawamura, K., and Fu, P.: Measurement report: Optical properties and sources of water-soluble brown carbon in Tianjin, North China – insights from organic molecular compositions, Atmos. Chem. Phys., 22, 6449–6470, https://doi.org/10.5194/acp-22-6449-2022, 2022.

Gao, Y., Wang, Q., Li, L., Dai, W., Yu, J., Ding, L., Li, J., Xin, B., Ran, W., and Han, Y.: Optical properties of mountain primary and secondary brown carbon aerosols in summertime, Sci. Total Environ., 806, 150570, https://doi.org/10.1016/j.scitotenv.2021.150570, 2022.

Gong, Y.: Dataset for "Measurement report: Brown Carbon Aerosol in Polluted Urban Air of North China Plain: Day-night Differences in the Chromophores and Optical Properties", Zenodo [data set], https://doi.org/10.5281/zenodo.7690230, 2023.

Hammer, M. S., Martin, R. V., van Donkelaar, A., Buchard, V., Torres, O., Ridley, D. A., and Spurr, R. J. D.: Interpreting the ultraviolet aerosol index observed with the OMI satellite instrument to understand absorption by organic aerosols: implications for atmospheric oxidation and direct radiative effects, Atmos. Chem. Phys., 16, 2507–2523, https://doi.org/10.5194/acp-16-2507-2016, 2016.

Harrison, M. A., Barra, S., Borghesi, D., Vione, D., Arsene, C., and Olariu, R. I.: Nitrated phenols in the atmosphere: a review, Atmos. Environ., 39, 231–248, 2005.

Hems, R. F. and Abbatt, J. P. D.: Aqueous Phase Photo-oxidation of Brown Carbon Nitrophenols: Reaction Kinetics, Mechanism, and Evolution of Light Absorption, ACS Earth Space Chem., 2, 225–234, https://doi.org/10.1021/acsearthspacechem.7b00123, 2018.

Hecobian, A., Zhang, X., Zheng, M., Frank, N., Edgerton, E. S., and Weber, R. J.: Water-Soluble Organic Aerosol material and the light-absorption characteristics of aqueous extracts measured over the Southeastern United States, Atmos. Chem. Phys., 10, 5965–5977, https://doi.org/10.5194/acp-10-5965-2010, 2010.

Huang, R.-J., Zhang, Y., Bozzetti, C., Ho, K.-F., Cao, J.-J., Han, Y., Daellenbach, K. R., Slowik, J. G., Platt, S. M., and Canonaco, F.: High secondary aerosol contribution to particulate pollution during haze events in China, Nature, 514, 218–222, 2014.

Huang, R.-J., Yang, L., Cao, J., Chen, Y., Chen, Q., Li, Y., Duan, J., Zhu, C., Dai, W., and Wang, K.: Brown carbon aerosol in urban Xi'an, Northwest China: the composition and light absorption properties, Environ. Sci. Technol., 52, 6825–6833, 2018.

Huang, R.-J., Wang, Y., Cao, J., Lin, C., Duan, J., Chen, Q., Li, Y., Gu, Y., Yan, J., Xu, W., Fröhlich, R., Canonaco, F., Bozzetti, C., Ovadnevaite, J., Ceburnis, D., Canagaratna, M. R., Jayne, J., Worsnop, D. R., El-Haddad, I., Prévôt, A. S. H., and O'Dowd, C. D.: Primary emissions versus secondary formation of fine particulate matter in the most polluted city (Shijiazhuang) in North China, Atmos. Chem. Phys., 19, 2283–2298, https://doi.org/10.5194/acp-19-2283-2019, 2019.

Huang, R. J., Yang, L., Shen, J., Yuan, W., Gong, Y., Guo, J., Cao, W., Duan, J., Ni, H., Zhu, C., Dai, W., Li, Y., Chen, Y., Chen, Q., Wu, Y., Zhang, R., Dusek, U., O'Dowd, C., and Hoffmann, T.: Water-Insoluble Organics Dominate Brown Carbon in Wintertime Urban Aerosol of China: Chemical Characteristics and Optical Properties, Environ. Sci. Technol., 54, 7836–7847, https://doi.org/10.1021/acs.est.0c01149, 2020.

Huang, R.-J., Yang, L., Shen, J., Yuan, W., Gong, Y., Ni, H., Duan, J., Yan, J., Huang, H., and You, Q.: Chromophoric Fingerprinting of Brown Carbon from Residential Biomass Burning, Environ. Sci. Technol. Lett., 9, 102–111, https://doi.org/10.1021/acs.estlett.1c00837, 2021.

Iinuma, Y., Böge, O., Gräfe, R., and Herrmann, H.: Methylnitrocatechols: atmospheric tracer compounds for biomass burning secondary organic aerosols, Environ. Sci. Technol., 44, 8453–8459, 2010.

Kampf, C. J., Jakob, R., and Hoffmann, T.: Identification and characterization of aging products in the glyoxal/ammonium sulfate system – implications for light-absorbing material in atmospheric aerosols, Atmos. Chem. Phys., 12, 6323–6333, https://doi.org/10.5194/acp-12-6323-2012, 2012.

Kasthuriarachchi, N. Y., Rivellini, L. H., Chen, X., Li, Y. J., and Lee, A. K. Y.: Effect of Relative Humidity on Secondary Brown Carbon Formation in Aqueous Droplets, Environ. Sci. Technol., 54, 13207–13216, https://doi.org/10.1021/acs.est.0c01239, 2020.

Kirchstetter, T. W., Novakov, T., and Hobbs, P. V.: Evidence that the spectral dependence of light absorption by aerosols is affected by organic carbon, J. Geophys. Res.-Atmos., 109, D21208, https://doi.org/10.1029/2004JD004999, 2004.

Kitanovski, Z., Grgić, I., Yasmeen, F., Claeys, M., and Čusak, A.: Development of a liquid chromatographic method based on ultraviolet–visible and electrospray ionization mass spectrometric detection for the identification of nitrocatechols and related tracers in biomass burning atmospheric organic aerosol, Rapid. Commun. Mass Sp., 26, 793–804, 2012.

Laskin, A., Laskin, J., and Nizkorodov, S. A.: Chemistry of atmospheric brown carbon, Chem Rev., 115, 4335–4382, https://doi.org/10.1021/cr5006167, 2015.

Li, J., Zhang, Q., Wang, G., Li, J., Wu, C., Liu, L., Wang, J., Jiang, W., Li, L., Ho, K. F., and Cao, J.: Optical properties and molecular compositions of water-soluble and water-insoluble brown carbon (BrC) aerosols in northwest China, Atmos. Chem. Phys., 20, 4889–4904, https://doi.org/10.5194/acp-20-4889-2020, 2020.

Li, X., Zhao, Q., Yang, Y., Zhao, Z., Liu, Z., Wen, T., Hu, B., Wang, Y., Wang, L., and Wang, G.: Composition and sources of brown carbon aerosols in megacity Beijing during the winter of 2016, Atmos. Res., 262, 105773, https://doi.org/10.1016/j.atmosres.2021.105773, 2021.

Lin, C., Huang, R.-J., Xu, W., Duan, J., Zheng, Y., Chen, Q., Hu, W., Li, Y., Ni, H., and Wu, Y.: Comprehensive Source Apportionment of Submicron Aerosol in Shijiazhuang, China: Secondary Aerosol Formation and Holiday Effects, ACS Earth and Space Chem., 4, 947–957, 2020.

Lin, P., Rincon, A. G., Kalberer, M., and Yu, J. Z.: Elemental Composition of HULIS in the Pearl River Delta Region, China: Results Inferred from Positive and Negative Electrospray High Resolution Mass Spectrometric Data, Environ. Sci. Technol., 46, 7454–7462, 2012.

Lin, P., Bluvshtein, N., Rudich, Y., Nizkorodov, S. A., Laskin, J., and Laskin, A.: Molecular Chemistry of Atmospheric Brown Carbon Inferred from a Nationwide Biomass Burning Event, Environ. Sci. Technol., 51, 11561–11570, https://doi.org/10.1021/acs.est.7b02276, 2017.

Liu, J., Lin, P., Laskin, A., Laskin, J., Kathmann, S. M., Wise, M., Caylor, R., Imholt, F., Selimovic, V., and Shilling, J. E.: Optical properties and aging of light-absorbing secondary organic aerosol, Atmos. Chem. Phys., 16, 12815–12827, https://doi.org/10.5194/acp-16-12815-2016, 2016.

Liu, S., Shilling, J. E., Song, C., Hiranuma, N., Zaveri, R. A., and Russell, L. M.: Hydrolysis of organonitrate functional groups in aerosol particles, Aerosol. Sci. Technol., 46, 1359–1369, 2012.

Liu, W.-J., Li, W.-W., Jiang, H., and Yu, H.-Q.: Fates of chemical elements in biomass during its pyrolysis, Chem. Rev., 117, 6367–6398, 2017.

Lu, C., Wang, X., Li, R., Gu, R., Zhang, Y., Li, W., Gao, R., Chen, B., Xue, L., and Wang, W.: Emissions of fine particulate nitrated phenols from residential coal combustion in China, Atmos. Environ., 203, 10–17, https://doi.org/10.1016/j.atmosenv.2019.01.047, 2019.

Lyu, R., Shi, Z., Alam, M. S., Wu, X., Liu, D., Vu, T. V., Stark, C., Fu, P., Feng, Y., and Harrison, R. M.: Insight into the composition of organic compounds ($\geq C_6$) in $PM_{2.5}$ in wintertime in Beijing, China, Atmos. Chem. Phys., 19, 10865–10881, https://doi.org/10.5194/acp-19-10865-2019, 2019.

Ni, H., Huang, R.-J., Pieber, S. M., Corbin, J. C., Stefenelli, G., Pospisilova, V., Klein, F., Gysel-Beer, M., Yang, L., and Baltensperger, U.: Brown carbon in primary and aged coal combustion emission, Environ. Sci. Technol., 55, 5701–5710, 2021.

Rogge, W. F., Hildemann, L. M., Mazurek, M. A., Cass, G. R., and Simoneit, B. R.: Sources of fine organic aerosol. 2. Noncatalyst and catalyst-equipped automobiles and heavy-duty diesel trucks, Environ. Sci. Technol., 27, 636–651, 1993.

Scaramboni, C., Urban, R. C., Lima-Souza, M., Nogueira, R. F. P., Cardoso, A. A., Allen, A. G., and Campos, M. D. M.: Total sugars in atmospheric aerosols: An alternative tracer for biomass burning, Atmos. Environ., 100, 185–192, 2015.

Schnitzler, E. G. and Abbatt, J. P. D.: Heterogeneous OH oxidation of secondary brown carbon aerosol, Atmos. Chem. Phys., 18, 14539–14553, https://doi.org/10.5194/acp-18-14539-2018, 2018.

Shen, R., Liu, Z., Chen, X., Wang, Y., Wang, L., Liu, Y., and Li, X.: Atmospheric levels, variations, sources and health risk of $PM_{2.5}$-bound polycyclic aromatic hydrocarbons during winter over the North China Plain, Sci. Total Environ., 655, 581–590, 2019.

Siemens, K., Morales, A., He, Q., Li, C., Hettiyadura, A. P., Rudich, Y., and Laskin, A.: Molecular Analysis of Secondary Brown Carbon Produced from the Photooxidation of Naphthalene, Environ. Sci. Technol., 56, 3340–3353, 2022.

Teich, M., van Pinxteren, D., Wang, M., Kecorius, S., Wang, Z., Müller, T., Močnik, G., and Herrmann, H.: Contributions of nitrated aromatic compounds to the light absorption of water-soluble and particulate brown carbon in different atmospheric environments in Germany and China, Atmos. Chem. Phys., 17, 1653–1672, https://doi.org/10.5194/acp-17-1653-2017, 2017.

Wang, H., Gao, Y., Wang, S., Wu, X., Liu, Y., Li, X., Huang, D., Lou, S., Wu, Z., and Guo, S.: Atmospheric processing of nitrophenols and nitrocresols from biomass burning emissions, J. Geophys. Res.-Atmos., 125, e2020JD033401, https://doi.org/10.1029/2020JD033401, 2020.

Wang, L., Wang, X., Gu, R., Wang, H., Yao, L., Wen, L., Zhu, F., Wang, W., Xue, L., Yang, L., Lu, K., Chen, J., Wang, T., Zhang, Y., and Wang, W.: Observations of fine particulate nitrated phenols in four sites in northern China: concentrations, source apportionment, and secondary formation, Atmos. Chem. Phys., 18, 4349–4359, https://doi.org/10.5194/acp-18-4349-2018, 2018.

Wang, Q., Han, Y., Ye, J., Liu, S., Pongpiachan, S., Zhang, N., Han, Y., Tian, J., Wu, C., and Long, X.: High contribution of secondary brown carbon to aerosol light absorption in the southeastern margin of Tibetan Plateau, Geophys. Res. Lett., 46, 4962–4970, 2019.

Wang, Y., Hu, M., Wang, Y., Zheng, J., Shang, D., Yang, Y., Liu, Y., Li, X., Tang, R., Zhu, W., Du, Z., Wu, Y., Guo, S., Wu, Z., Lou, S., Hallquist, M., and Yu, J. Z.: The formation of nitro-aromatic compounds under high NO_x and anthropogenic VOC conditions in urban Beijing, China, Atmos. Chem. Phys., 19, 7649–7665, https://doi.org/10.5194/acp-19-7649-2019, 2019.

Wang, X., Gu, R., Wang, L., Xu, W., Zhang, Y., Chen, B., Li, W., Xue, L., Chen, J., and Wang, W.: Emissions of fine particulate nitrated phenols from the burning of five common types of biomass, Environ Pollut., 230, 405–412, https://doi.org/10.1016/j.envpol.2017.06.072, 2017.

Xie, C., Xu, W., Wang, J., Wang, Q., Liu, D., Tang, G., Chen, P., Du, W., Zhao, J., Zhang, Y., Zhou, W., Han, T., Bian, Q., Li, J., Fu, P., Wang, Z., Ge, X., Allan, J., Coe, H., and Sun, Y.: Vertical characterization of aerosol optical properties and brown carbon in winter in urban Beijing, China, Atmos. Chem. Phys., 19, 165–179, https://doi.org/10.5194/acp-19-165-2019, 2019.

Xue, X., Zeng, M., and Wang, Y.: Highly active and recyclable Pt nanocatalyst for hydrogenation of quinolines and isoquinolines, Appl. Catal. A-Gen., 560, 37–41, 2018.

Yuan, B., Liggio, J., Wentzell, J., Li, S.-M., Stark, H., Roberts, J. M., Gilman, J., Lerner, B., Warneke, C., Li, R., Leithead, A., Osthoff, H. D., Wild, R., Brown, S. S., and de Gouw, J. A.: Secondary formation of nitrated phenols: insights from observations during the Uintah Basin Winter Ozone Study (UBWOS) 2014, Atmos. Chem. Phys., 16, 2139–2153, https://doi.org/10.5194/acp-16-2139-2016, 2016.

Yuan, W., Huang, R.-J., Yang, L., Guo, J., Chen, Z., Duan, J., Wang, T., Ni, H., Han, Y., Li, Y., Chen, Q., Chen, Y., Hoffmann, T., and O'Dowd, C.: Characterization of the light-absorbing properties, chromophore composition and sources of brown carbon aerosol in Xi'an, northwestern China, Atmos. Chem. Phys., 20, 5129–5144, https://doi.org/10.5194/acp-20-5129-2020, 2020.

Yuan, W., Huang, R.-J., Yang, L., Wang, T., Duan, J., Guo, J., Ni, H., Chen, Y., Chen, Q., Li, Y., Dusek, U., O'Dowd, C., and Hoffmann, T.: Measurement report: $PM_{2.5}$-bound nitrated aromatic compounds in Xi'an, Northwest China – seasonal variations and contributions to optical properties of brown carbon, Atmos. Chem. Phys., 21, 3685–3697, https://doi.org/10.5194/acp-21-3685-2021, 2021.

Zhan, Y., Li, J., Tsona, N. T., Chen, B., Yan, C., George, C., and Du, L.: Seasonal variation of water-soluble brown carbon in Qingdao, China: Impacts from marine and terrestrial emissions, Environ. Res., 212, 113144, https://doi.org/10.1016/j.envres.2022.113144, 2022.

Zhang, S., Zhang, W., Wang, K., Shen, Y., Hu, L., and Wang, X.: Concentration, distribution and source apportionment of atmospheric polycyclic aromatic hydrocarbons in the southeast suburb of Beijing, China, Environ. Monit. Assess., 151, 197–207, 2009.

Zhang, Y. and Hatakeyama, S.: New directions: Need for better understanding of source and formation process of phthalic acid in aerosols as inferred from, Atmos. Environ., 140, 147–149, https://doi.org/10.1016/j.atmosenv.2016.05.058, 2016.